Available online at www.sciencedirect.com
ScienceDirect
Catalysis Today 122 (2007) 27–38
CATALYSIS TODAY
www.elsevier.com/locate/cattod

Oxidation of nauseous sulfur compounds by photocatalysis or photosensitization

C. Cantau [a], S. Larribau [a], T. Pigot [a], M. Simon [a], M.T. Maurette [b], S. Lacombe [a,*]

[a] *Laboratoire de Chimie Théorique et de Physico-Chimie Moléculaire, UMR CNRS 5624, FR 2606, Faculté des Sciences, BP 1155, 64013 PAU Cedex, France*

[b] *Laboratoire des IMRCP, UMR CNRS 5623, Université Paul Sabatier, 118 route de Narbonne, 31062 Toulouse Cedex 4, France*

Available online 1 February 2007

Abstract

Reduced sulfur compounds such as methanethiol (MSH), dimethylsulfide (DMS) and dimethydisulfide (DMDS) are nauseous by-products produced by a great number of industrial processes. Oxidation of these reduced sulfur compounds in polluted atmospheres and hence the decrease of their harmful and malodorous effects is thus a matter of concern in numerous industrial and water treatment plants. Photocatalytic treatment of gaseous flow polluted by these sulfur compounds has been actively investigated for the last few years.

The first part of the paper is devoted to a literature review on the different TiO_2-based photocatalytic processes designed for the oxidation of these gaseous compounds. The comparison of their efficiency is done according to the process parameters: batch or flow reactors, photocatalytic materials, residence time, gas flow, pollutant nature and concentration, relative humidity, ... Special attention is paid to the poisoning of the photocatalytic material and to its possible recycling.

In the second part of the paper, alternative materials based on aromatic photosensitizers (9,10-dicyanoanthracene, 9,10-anthraquinone) deposited or grafted on silica matrices are then presented and their efficiency compared to more conventional TiO_2-based materials. It is demonstrated that the oxidation products are totally different from those obtained with TiO_2. With the photosensitizing materials, singlet oxygen addition is shown to be the major pathway, leading to sulfoxide and sulfone starting from DMS and to methyl methanethiosulfonate starting from DMDS. With TiO_2-based materials, in the absence of water and hence of hydroxyl radicals, products arising of C–S and S–S bond cleavage are mainly obtained: disulfide from DMS and CH_3SSSCH_3 together with $CH_3SCH_2SSCH_3$ from DMDS. These latter products may be accounted for by electron transfer from sulfide or disulfide to photogenerated holes, leading to radical mechanisms. Mineralization to CO_2 and H_2O is also shown to occur with DMS, but is not favoured under these conditions, due to the absence of water and of a too fast gas hourly space velocity (GHSV).

The advantages–drawbacks of the two kinds of materials are presented.

Keywords: Reduced sulfur compounds; Photooxidation; Photosensitization; Gas–solid reactions; Supported photocatalysts

1. Introduction

Reduced sulfur compounds such as methanethiol (MSH), dimethylsulfide (DMS) and dimethyldisulfide (DMDS) are nauseous by-products issued from energy production technologies, chemical plants, tanneries, food processing operations, pulp and paper mills, as well as from aerobic or anaerobic waste water treatment plants, composting plants and rendering plants. In the particular case of Kraft pulp mills, the reduction of nauseous reduced sulfur gases is achieved by incineration of condensed sources, but the treatment of diluted, diffuse surface sources appears to be more difficult. For example, 94 ppmv of methanethiol, 17 ppmv of DMS and 22 ppmv of DMDS were measured in gas effluents of the Kraft paper pulping process [1]. The oxidation of these reduced sulfur compounds in polluted atmospheres and hence the decrease of their malodorous effects is thus a matter of concern in numerous industrial and water treatment plants.

Photocatalytic oxidation of numerous organic compounds in the gas phase has been developed rather recently relative to water photocatalytic treatment and proved to be efficient in several cases [2–4]. In such gas phase photocatalytic oxidation,

* Corresponding author. Tel.: +33 559 407 579; fax: +33 559 407 451.
E-mail address: sylvie.lacombe@univ-pau.fr (S. Lacombe).

0920-5861/$ – see front matter © 2007 Elsevier B.V. All rights reserved.
doi:10.1016/j.cattod.2007.01.038

air is the only chemical oxidant, the reactions generally work under ambient pressure at room temperature and activation is provided by low-energy light (UV-A). These advantages make photocatalytic treatment of gaseous pollutants worth studying, although the main drawback of this process is related to the poisoning of the generally used titanium dioxide (TiO_2) photocatalyst.

Since this topic has been only recently investigated by several authors, one of the aims of this paper is to present an overall review on the last published results in the field of photocatalytic oxidation of reduced sulfur compounds. The second part is devoted to a summary of our own experimental results obtained with original materials on dimethysulfide (DMS) and dimethyldisulfide (DMDS) photocatalytic removal.

2. Literature review on photocatalytic oxidation of reduced sulfur compounds

The photocatalytic oxidation of gaseous alkyl sulfides has been found to proceed over TiO_2 materials under ambient conditions [5–11], while the problem of the photocatalytic decomposition of other malodorous sulfur compounds has been less addressed [12,13]. Photooxidation of gaseous dimethylsulfide (DMS) or diethylsulfide (DES) has been studied in flow [6,7,14] or batch reactors [15]. In a flow reactor, diethylsulfide (concentration: 368 ppmv, flow rate: 20 $cm^3\ min^{-1}$, residence time: unknown) was shown by Vorontsov et al. [7] to be converted on different TiO_2 samples in numerous gaseous (diethyldisulfide, acetaldehyde, ethanol, carbon dioxide) or adsorbed products (diethyldi- and trisulfide, diethylsulfoxide, diethylsulfone, ...) and product distribution appeared to be dependant upon humidity, light intensity, and addition of hydrogen peroxide in the gas flow. The catalysts showed deactivation with a characteristic temporal range of 100–300 min. The catalyst deactivation was studied and its reactivation carried out by the same research group in a larger volume flow reactor (250 ml, flow rates between 55 and 1100 $cm^3\ min^{-1}$, residence time: between 11 and 272 s) [14]. Deactivation, expressed by decrease of effluent CO_2 concentration and appearance of gaseous intermediates, was shown to be related to adsorbed sulfates formed during the course of oxidation and deactivation rate was dependant on water concentration, catalyst loading and feed DES concentration. Indeed, moderately low feed water concentration (1900 ppmv, 8% relative humidity or RH) provided the highest photocatalytic activity for DES destruction in this coil reactor and hence the lowest deactivation rate. The better way to reactivate the catalyst was the cycle ''irradiation–water washing–drying'', although some permanent catalyst deactivation was noted. Some prominent results of these two studies include the importance of the adsorption step on the conversion of DES and the change in product distribution with longer residence time. It is worth noting that according to Kozlov et al. [15], in a batch reactor at 30% RH, DES is converted to acetaldehyde and ethylene (in the gas flow) and diethylsulfone and carboxylates (adsorbed on the catalyst) as intermediates, while the final oxidation products are carbon dioxide, water and adsorbed sulfate species responsible for catalyst deactivation.

The photocatalytic degradation of gaseous DMS in a flow reactor (concentration: 154 ppmv, flow rate: 375 $cm^3\ min^{-1}$, residence time: evaluated around 37 s) using dry synthetic air was also shown by Peral et al. [6] to be highly dependant on catalyst deactivation. Methanol, dimethylsulfoxide (DMSO) and CO_2 were detected as oxidation products in the gas phase, as well as adsorbed oxidized species on the catalyst, tentatively identified as sulfone, sulfoxide and sulfates. No mention to the formation of dimethyldisulfide was made in this latter study.

The literature data presented above illustrate the ability of TiO_2 photocatalysis to oxidize sulfides. However, no clear-cut conclusion can be made on the effect of the different process parameters (flow rate, gas residence time, reactor form, pollutant inlet concentration, relative humidity, radiant emittance, ...). Very recently, Demeestere et al. [16] have carried out such a systematic research on the effect of these process parameters on pollutant removal efficiency, catalyst deactivation and reaction product distribution in a flow reactor with TiO_2 Degussa P25 as photocatalyst. Their results prove that DMS inlet concentration is the main crucial factor accounting for catalyst deactivation. Moreover, they confirm that catalyst deactivation is the consequence of accumulation of reaction products on the surface and this effect is less pronounced at lower RH and with higher gas residence time. DMDS, SO_2, CO_2 were detected as oxidation products in the gas phase. Moreover, desorption of the photocatalyst revealed the presence of adsorbed dimethylsulfoxide, dimethylsulfone, methanesulfonic acid and sulfate. They also noted that DMS inlet concentration had no effect on the distribution of the oxidation products, in contrast to RH. Indeed, the formation of dimethylsulfone, methanesulfonic acid and CO_2 was favoured at higher RH while DMDS was the main reaction product at lower RH.

In a following work, Demeestere et al. [17] focused their attention on DMS degradation with modified TiO_2 under daylight irradiation. Actually, it is well known that another hot topic in photocatalysis concerns the synthesis of new TiO_2 materials in order to convert the TiO_2 absorption onset from ultraviolet to the visible region by for example anionic doping with non-metal elements such as N [18–25], C [26–28] and S [29,30]. In contrast to these anion doped TiO_2 photocatalysts, S-cation doped TiO_2 was recently prepared using a sol–gel method by Ohno et al. [31] (S–TiO_2–SG). This material was chosen by Demeestere et al. [17] to study its efficiency on visible light mediated gaseous DMS degradation, since data on photocatalytic activity in the gas phase are scarce and even missing for sulfides, as these modified photocatalysts are more usually used in solution. Another S-doped TiO_2 material, prepared through physical mixture of TiO_2 powder and thiourea in an agate mortar (S–TiO_2–PM), was also investigated in this work and compared to the ''Ohno'' photocatalyst. These experiments were performed in a cylindrical borofloat glass batch reactor (volume: 32 ml) and were carried out at three different gas-phase equilibrium concentrations ranging from 104 to 537 ppmv and at RH 21 ± 2% (this humidity level was

shown to be optimal towards photocatalytic DMS degradation kinetics [16]) with 25 mg of photocatalyst powder under daylight irradiation. The results revealed that under these reaction conditions, S–TiO_2–PM was the best catalyst in regard of its highest activity towards DMS degradation. Even at concentrations up to 537 ppmv, removal efficiencies higher than 99% were obtained within 120 min irradiation. Moreover, the authors observed a slower carbon mineralization, accounted for by the formation of intermediate products, such as DMDS, sole intermediate detected in the gas phase, in agreement with their previous work [16] and with our own observations with unmodified TiO_2 [32].

These recent literature data mostly deal with DMS or DES removal whereas studies about disulfide and thiol photooxidations are scarcer.

The photocatalytic oxidation of dimethyldisulfide (DMDS) was carried out by Canela et al. [12] in a flow reactor (concentration 34 ppmv, flow rate 474 $cm^3\ min^{-1}$, residence time 51 s, RH 23%) and led to its complete conversion to gaseous carbon dioxide and sulfur dioxide and to adsorbed sulfate, without any catalyst deactivation. In an attempt to prepare adsorbing photocatalysts based on SiO_2/TiO_2 powder materials, Nishikawa and Takahara [13] observed the oxidation of DMS and DMDS in a flow reactor for different residence times (27, 54 and 107 s). Whatever the residence time, DMS oxidation was complete over the catalyst with the best adsorption capacity (50 $\mu g\ g^{-1}$ for DMS and 116 $\mu g\ g^{-1}$ for DMDS), while DMDS degradation was only 50% for the highest residence time (107 s). The sole gaseous product from DMS oxidation was sulfur dioxide, together with adsorbed formic and acetic acid, without any formation of DMDS on this particular catalyst. Starting from DMDS, gaseous sulfur dioxide and formic acid were detected, together with adsorbed formic and acetic acid, just like in the DMS case. No indication about relative humidity was given in this paper.

Up to now, mercaptans (thiols) removal has been investigated by catalytic oxidation, adsorption–oxidation on activated carbons, catalytic incineration and also some biological alternative processes. To the best of our knowledge, the oxidation of methyl mercaptan (CH_3SH) by TiO_2 photocatalysis has been studied by Li et al. [33]. Their experiments were conducted in a batch photoreactor with an effective volume of 33.4 l. The photocatalyst was deposed by coating on a glass fiber sheet. NH_4^+-modified TiO_2 photocatalyst and SO_4^{2-}-modified TiO_2 photocatalyst were prepared by a hydrothermal method and their activity on CH_3SH degradation was compared to those of commercial TiO_2 Degussa P25 with an initial CH_3SH concentration of 94 ppmv and a relative humidity of 60% at room temperature with conventional 350 nm irradiation. From their results, NH_4^+-modified TiO_2 photocatalyst was more efficient than TiO_2 Degussa P25, whereas SO_4^{2-}-modified TiO_2 photocatalyst was less efficient. The authors concluded that the high photocatalytic activity of NH_4^+-modified TiO_2 photocatalyst resulted both from its basic properties and enhanced specific surface area relative to commercial TiO_2. This work also focused on the influence of process parameters like catalyst loading, relative humidity and inlet CH_3SH concentration. The results revealed that a catalyst loading of 3.93 mg cm^{-2} and a RH of 43% were two essential factors for achieving the best performance. The kinetic data at different CH_3SH inlet concentration were fitted with a pseudo-first order model. The photocatalytic degradation of CH_3SH and H_2S was also performed using a silver-deposited TiO_2 photocatalysts by Kato et al. [34] since it is well know that SH functional group in sulfides adsorbs on gold and silver strongly [35–37] and that the deposition of metals (such as platinum, gold, palladium and silver) on TiO_2 increases the charge separation efficiency and inhibits recombination of photoinduced electron and hole. In this study, the photocatalyst was placed at the center of a stainless steel reactor (0.15 l) with a cover quartz window (thickness 3 mm). Experiments were carried out flowing 0.75 ppmv of thiol or H_2S through the reactor at a flow rate of 3 $dm^3\ min^{-1}$ (at room temperature). The photocatalytic degradation of CH_3SH and H_2S was significantly improved by using this silver-deposited TiO_2 photocatalyst, while sulfur atoms were oxidized into sulfate ion and accumulated on the photocatalyst.

It should also be recalled that H_2S photooxidation was shown to occur over TiO_2 only in the presence of oxygen. Canela et al. [38] have analyzed H_2S decomposition using TiO_2 with UV light in a gas flow reactor (flow rate: 164–1500 $cm^3\ min^{-1}$, residence time: 16–148 s). They showed the presence of sulfates (SO_4^{2-}) on TiO_2 without any deactivation of the catalyst up to concentration of 600 ppmv, with a mass balance around 95% towards formation of sulfate anion. This work left some remaining questions concerning first, whether the reaction occurred on the TiO_2 surface and second, on the reaction pathway for conversion of sulfides to sulfates. Thus, the photocatalytic oxidation of H_2S at the gas–solid interface using TiO_2 as photocatalyst was also investigated by Kataoka et al. [39]. Photocatalytic oxidation kinetic studies were carried out using a small vial-type reactor. By coupling analysis of gas samples by GC–MS with XPS analysis of the surface of TiO_2 photocatalyst, they determined that H_2S was oxidized to SO_4^{2-} without producing gaseous intermediates. Moreover, the use of in situ diffuse reflectance and in situ transmission FT-IR spectroscopy provided further detail about this reaction. First, sulfates gradually accumulated on the TiO_2 surface during the reaction and second, SO_2^- was one possible intermediate.

In summary, photooxidation of reduced sulfur compounds has been mainly carried out with TiO_2-based photocatalysts under UV irradiation. Despite the various operating conditions depending on research groups, the collected data put forward some essential parameters concerning the photooxidation efficiency (relative humidity (RH) of the gaseous effluent, residence time, inlet concentration of pollutant, photocatalyst charge), which should be optimized on each photocatalytic reactor for improving pollutant removal. For example, the optimal relative humidity is higher for CH_3SH than for DMS. It also appears that the photooxidation products reported by the different authors are not always the same. Starting from sulfides, formation of sulfoxides,

sulfones, disulfides, aldehydes, carbon dioxide and sulfur dioxide are alternatively observed, while sulfates and carboxylates always adsorb on the catalyst. The only studied disulfide is DMDS, which gives rise upon photooxidation to carboxylic acids and SO_2. H_2S is converted into sulfates, while there are almost no data on thiols. The main drawback or limitation of TiO_2-based photocatalyts is related to their deactivation following accumulation of organic products and mainly of sulfates on their surface during mineralization of pollutant. Nevertheless, this deactivation seems less important with lower RH, lower inlet pollutant concentration and higher residence time.

Several studies focus on modified TiO_2 photocatalyst either with metals (to prevent the electron–hole recombination) or with heteroelements such as N, C and S (to shift the TiO_2 absorption onset to the visible region). Although these modified TiO_2 give promising results, no definitive conclusion can be drawn at the moment and further developments are obviously needed. Adsorption of the pollutant being an essential step, coupling in the same process materials with high adsorption capacity and photocatalytic activity could also improve the overall efficiency.

3. New materials designed for the oxidation of reduced sulfur compounds

In an attempt to design new materials for the photocatalytic degradation of reduced sulfur compounds of interest in Kraft paper mills, we describe in the following our own results on the photooxidation of DMS and DMDS with three different photocatalysts. Compared to the previously described photocatalytic materials, our investigations focused at the efficiency of strikingly different materials, based on aromatic photosensitizers supported on silica. While sensitizers like phthalocyanines [40,41], 9,10-dicyanoanthracene [42] or benzophenone [43] derivatives immobilized on silica were already used in solution, and were shown to produce activated oxygen species, their application to gas phase oxidation is scarcer [44]. Another point worth interest is their possible activation by visible light.

In order to be efficient at the gas–solid interface, such materials must answer the following criteria: they have to be conveniently handled in a gas flow reactor, must be transparent, and porous. Silica monoliths correspond to these criteria.

The first material studied in the following was a silica monolith prepared by a sol–gel (SG) method where a photosensitizer was incorporated [44]. 9,10-Dicyanoanthracene (DCA) was chosen as the photosensitizer owing to its high efficiency for sulfide oxidation in solution [42,43,45]. The corresponding highly porous and transparent monoliths are called DCA-SG in the following.

The second one was an original material prepared by grafting an anthraquinone (ANT) derivative on commercial silica beads. Contrary to the previous material, the sensitizer was not adsorbed but covently bound on the silica surface. Anthraquinone was chosen as the sensitizer first because of its high efficiency for sulfide oxidation in solution [45] or in the gas phase [44], and second, because a graftable anthraquinone derivative was easily synthesized. This material is called ANT-SB in the following.

The efficiency of these two materials was compared with that of a more conventional one, based on TiO_2 deposited by the sol–gel method on quartz supports (TiO_2-QZ), already described and used for the oxidation of different organic compounds (alcohols, amines, aromatics and sulfides) [32,46,47].

It should be noted that in this preliminary study, neither the catalyst packing in the reactor, nor the material mass, and hence the residence time of pollutant on the material, were optimized. These experiments were aimed at the comparison of photooxidation efficiency of these three materials in a flow reactor under similar conditions.

4. Experimental

The preparation of DCA-SG [44] and TiO_2-QZ [46,47] was already described. ANT-SB catalyst was prepared by grafting a triethoxysilyl derivative **3** of anthraquinone 2-carboxylic-acid **1** on silica gel beads (ACROS, 3–6 mm, pore diameter ca. 9 nm, specific surface area 400 $m^2\ g^{-1}$).

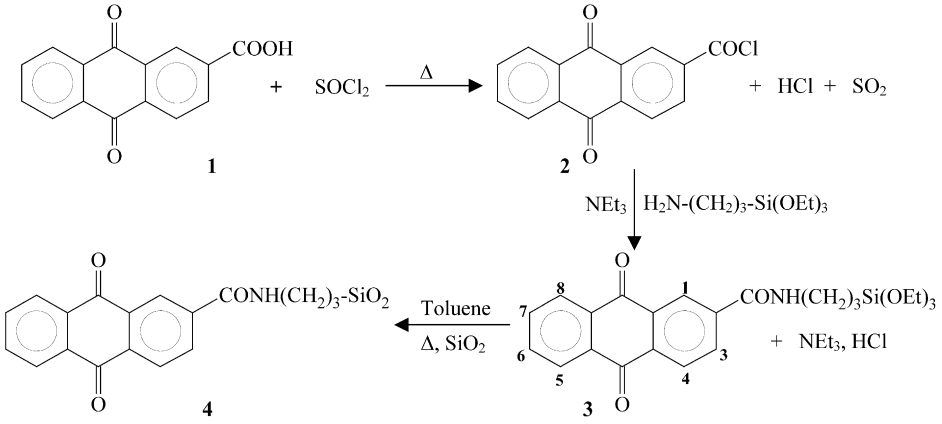

One gram (3.9 mmoles) of **1** was dissolved in the minimum amount of $SOCl_2$ added dropwise with a syringe under N_2. The mixture was heated at 110 °C for 3 h. The formation of acid chloride **2** was controlled by IR spectroscopy since the band at 1680 cm^{-1} (υ_{CO} COOH) was replaced by a band at 1780 cm^{-1} (υ_{CO} COCl). The melting point of the acid chloride **2** was 143 °C.

Excess $SOCl_2$ was removed by flushing with N_2 and the acid chloride was dissolved in 10 ml of dry toluene. Then 3-aminopropyltriethoxysilylane (APTES, Fluka) (4.3 mmoles, 1 ml) and NEt_3 (4.3 mmoles, 0.6 ml) were simultaneously added to the toluene solution of **2** with two microsyringes. The mixture was stirred for 2 h at room temperature. Released HCl precipitated as triethylamine hydrochloride. Successive precipitations and filtrations of NEt_3, HCl were achieved in chloroform–hexane, or ether–hexane mixtures. The soluble amide **3** was then recovered by solvent evaporation and recrystallized in hexane.

2-Carbamoyl-(*N*-propyl-3-triethoxysilane)anthraquinone **3**: *F* 193 °C; IR (KBr): 3297 (broad), 2970, 2924, 2855, 1673, 1638 cm^{-1}; UV, ε_{327nm}: 5650; ^{1}H NMR ($CDCl_3$): δ 8.61 (s, 1H, $\mathbf{H_1}$), 8.4 (d, 2H, $\mathbf{H_{3-4}}$), 8.34 (t, 2H, $\mathbf{H_{5-8}}$), 7.8 (t, 2H, $\mathbf{H_{7-6}}$), 7.28 (s, 1H, **NH**), 3.87 (q, 6H, O–$\mathbf{CH_2}$–CH_3), 3.7 (t, 2H, NH–$\mathbf{CH_2}$–), 1.43 (td, 2H, –$\mathbf{CH_2}$–CH_2–Si), 1.26 (m, 9H, CH_2–$\mathbf{CH_3}$), 0.76 (t, 2H, $\mathbf{CH_2}$–Si).

For its grafting on silica, the amide **3** (0.5 mmoles g^{-1} of silica) was dissolved in toluene and added dropwise under nitrogen on the silica beads previously dried under primary vacuum at 200 °C for 6 h and then for 12 h at ambient temperature. The mixture was kept 1 h at room temperature and then heated for 14 h under reflux. The synthesized material was filtered, washed with dichloromethane–ether (50–50) in a Soxhlet extractor and dried under vacuum at 100 °C. The amount of grafted amide **3** was deduced from the UV analysis of filtrated toluene (determination of non-grafted **3**). The grafting ratio was then confirmed by microanalysis based on nitrogen determination (found: 0.40, i.e. 2.8×10^{-4} moles g^{-1} silica), by thermogravimetric analysis (TGA) (2.5×10^{-4} moles g^{-1} silica), and by DRUV (2.8×10^{-4} moles g^{-1} silica) after calibration of the diffuse reflectance spectra on adsorbed anthraquinone. NMR ^{29}Si spectrum of **4** showed the characteristic *T* site at about −40, −50 ppm indicating chemical bond between silica beads and **3**.

Nitrogen adsorption and desorption isotherms of the materials were measured at 77 K on a Micromeritics ASAP 2010 Micropore nitrogen adsorption apparatus. Thermogravimetric experiments were carried out on a TGA model 2950 under N_2 flow. Before nitrogen adsorption and desorption experiments, samples were dried at 150 °C under 10 μmHg for 24 h (it was verified by diffuse reflectance UV (DRUV) that with this drying treatment, no sensitizer consumption occurred). DRUV spectra of the ground materials were recorded on a Varian Cary 5 spectrometer with a 110 mm PTFE integrating sphere [48]. The reflectance spectra were corrected against a Teflon standard reflectance spectrum.

The scheme of the single-path flow reactor has already been described [44]. The gas outlet was directly sampled by a pneumatic valve located on the injection port of a VARIAN 3800 chromatograph equipped with a Chrompack column CPSil-5CB (30 m, 0.25 mm, 1 μm). The gas flow was analyzed every 10 min and the concentration of pollutant or of its oxidation products was thus followed over the whole experiment, after identification of the oxidation products by comparison with pure standards or analysis by GC–MS. Alternatively, a Varian CP-4900 micro-GC with a thermal conductivity detector may be used to detect sulfur dioxide, carbon dioxide or water in the effluent. Before switching on the lamps, the saturation of the sample by the pollutant was performed in order to reach the adsorption equilibrium and hence the amount of adsorbed pollutant.

During irradiation, the components of the gas flow may eventually be concentrated on a Carboxen SPME fiber, which was then desorbed in the injector of a HP 5973 GC–MS chromatograph (column SPB35, 60 m, 0.32 mm, 1 μm) for

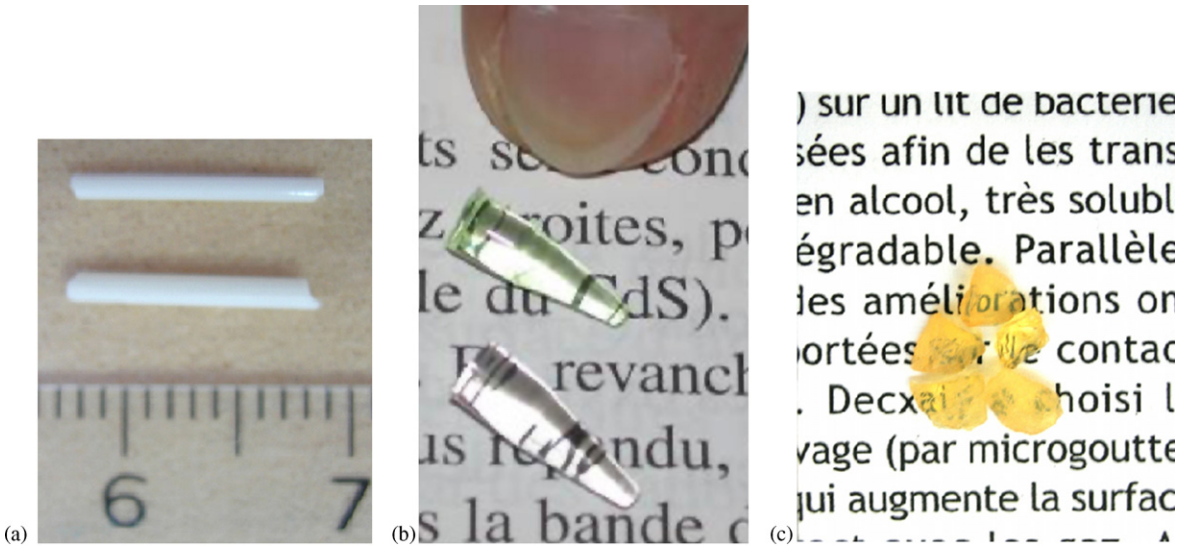

Fig. 1. Photos of (a) TiO_2-QZ bars; (b) (top) a DCA-SG monolith; (bottom) a non-doped monolith; (c) ANT-SB beads.

analysis and identification of the unknown oxidation products. Finally, the materials after irradiation were separated in two sets: the first was sonicated for 30 min in dichloromethane, and the second in deionized water. The dichloromethane solution was analyzed by GC for identification of desorbed organic products, while the aqueous extract was analyzed by ion exchange chromatography (IEC) in the suppressed conductivity mode on a Dionex DX-20 chromatograph equipped with an AS9-HC (4 mm) column.

Radiometric measurements were performed with an ORIEL photodiode OPM^{TM} detector (size 10 mm × 10 mm) equipped with an OPM^{TM} multifunction optical powermeter. The radiant emittance in the photoreactor was 14 mW cm^{-2} for the set of 15 RPR-4190 lamps and 12.7 mW cm^{-2} for the set of 15 RPR-3500 lamps.

5. Results

5.1. Characterization of the materials

The different materials are presented in Fig. 1 and their characteristics are summarized in Table 1.

The TiO_2-based materials (TiO_2-QZ) are small tubular white bars (Fig. 1a) with a weak specific surface area (80 m^2 g^{-1}) and are mostly mesoporous. The DRUV spectrum of ground TiO_2-QZ is given in Fig. 2 (curve (a)) and, as expected, this material absorbs weakly in the UV-A range.

DCA-SG [32] are small transparent cones (Fig. 1b) with a DCA concentration around 2.1×10^{-7} mol g^{-1} (the low solubility of DCA in methanolic solution used in the sol–gel synthesis limits DCA concentration in the material at this upper concentration). Its specific surface area is 1170 m^2 g^{-1} with an adsorption isotherm characteristic of a microporous material with 21% of mesoporous surface. The DRUV spectrum of the ground samples (Fig. 2, curve (b)) displays the characteristic feature of the DCA moiety in the 376–422 nm range and hence these materials may be activated by visible light. From their emission spectra, it was concluded that only DCA monomer is present, without any excimer formation, in agreement with the low DCA concentration in the silica sol–gel [32].

ANT-SB are small transparent yellow beads (Fig. 1c) with an anthraquinone loading around 2.8×10^{-4} mol g^{-1} according to TGA and DRUV analysis. Relative to the previously described DCA-SG, higher ANT concentration is needed due to the much lower molar extinction coefficient at 420 nm of ANT relative to DCA. Their specific surface area is 260 m^2 g^{-1} with an adsorption isotherm characteristic of a microporous material with 30% of mesoporous surface. The

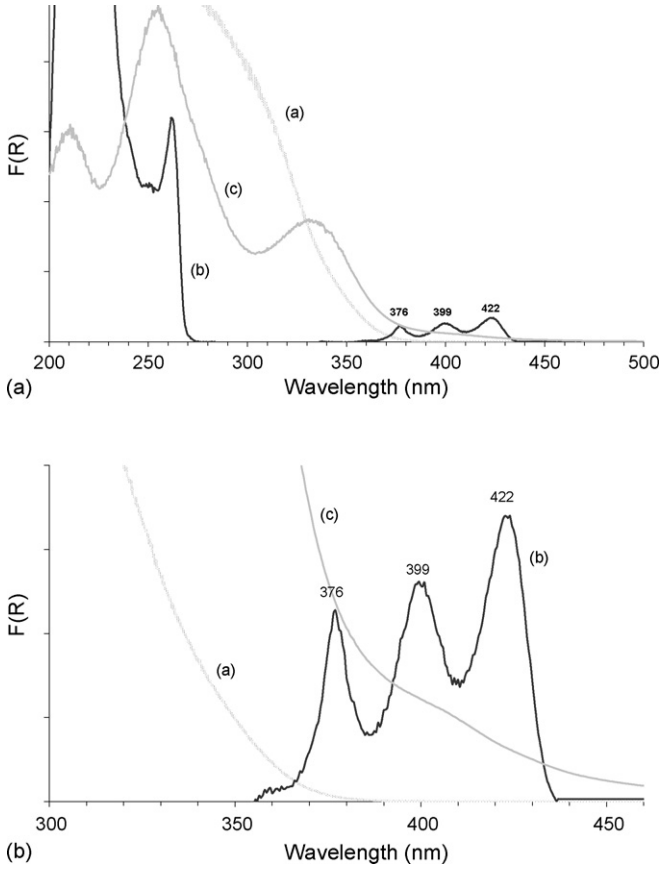

Fig. 2. (a) DRUV spectra (200–500 nm) of (a) TiO_2-QZ, (b) DCA-SG and (c) ANT-SB before irradiation; (b) zoom (300–460 nm) of the same DRUV spectra.

DRUV spectrum of the ground samples (Fig. 2, curve (c)) displays the characteristic feature of the anthraquinone moiety with a noticeable absorption from the UV range to 450 nm. Hence, these materials may be activated by visible light like DCA-SG.

The amount of adsorbed DMS and DMDS at the equilibrium concentration for the three materials was compared from the study of the pollutant concentration evolution with time (i.e. the breakthrough curves) in the dark [32]. The results are given in Table 1. DCA-SG (146 mg g^{-1} for DMS and 131 mg g^{-1} for DMDS) displays the best adsorption capacity relative to ANT-SB (10 mg g^{-1} for DMS and 24 mg g^{-1} for DMDS) and TiO_2-QZ (14 mg g^{-1} for DMS and 18 mg g^{-1} for DMDS), in agreement with the respective specific surface area of the materials, although the amount of DMS adsorbed by ANT-SB appears smaller than expected. Moreover, it may be noted that DMDS adsorption capacity of each material is close to their DMS adsorption capacity.

Table 1
Characteristics of the materials used for the photooxidation experiments (PS for photosensitizer)

	Specific surface area (m^2 g^{-1})	PS or TiO_2 concentration (mol g^{-1})	DMS adsorption (mg g^{-1})	DMDS adsorption (mg g^{-1})
TiO_2-QZ	80	1.25×10^{-3}	14	18
ANT-SB	260	2.8×10^{-4}	10	24
DCA-SG	1170	2.1×10^{-7}	146	131

Table 2
Efficiency for DMS removal of each photocatalyst under various conditions

Entry	Photocatalyst used	Irradiation wavelength (nm)	Flow rate (ml min^{-1})	Gas hourly space velocity (GHSV) (h^{-1})	DMS concentration (ppmv)	% DMS abatement
1	DCA-SG, 0.6 g	420	67	2250	100	90
2	DCA-SG, 0.6 g	420	10	333	400	98
3	ANT-SB, 2 g	420	67	563	100	98
4	TiO_2-QZ, 0.6 g	350	10	167	400	30

5.2. Photocatalytic results

We present in the following the results of photooxidation of DMS and DMDS with these three materials. First, no photooxidation of DMS or DMDS occurred through photolysis in the absence of material, as expected from the lack of absorption band for these compounds at wavelengths longer than 250 nm.

5.2.1. DMS

The reactor was loosely packed with the photocatalytic materials. When the adsorption equilibrium was reached, the photooxidation efficiency of the three materials was compared under various conditions. For the purpose of comparison, all the following experiments were carried out for the same irradiation time (120 h). After the adsorption step of DMS in the dark, the DMS drop (% abatement) was evaluated by the ratio of removed DMS (deduced from the integration of its break-through curve under irradiation) to the total entering flow of DMS. The results are reported in Table 2. Owing to their DRUV spectra, TiO_2-QZ was irradiated at 350 nm (15 RPR-3500 lamps) whereas DCA-SG and ANT-SB were activated at 420 nm (15 RPR-4200 lamps). Under these conditions, DCA-SG and ANT-SB catalysts showed the best activity for DMS abatement. Focusing to experiments with DCA-SG (Entries 1 and 2), the gas hourly space velocity (GHSV) [49] appeared to be a crucial parameter: despite a 4-fold higher DMS concentration but a 7-fold decrease of the GHSV, an increased abatement (98%) is observed. In spite of a lower GHSV, the DMS removal with TiO_2-QZ was less efficient (30% abatement, Entry 4). ANT-SB, as DCA-SG, thus shows an actual efficiency for DMS removal (98%) although, as shown in Table 1, the concentration of photoactive molecules in TiO_2-QZ (1.25×10^{-3} mol g^{-1}) was higher than that in ANT-SB (2.8×10^{-4} mol g^{-1}) or DCA-SG (2.1×10^{-7} mol g^{-1}).

Organic and inorganic products, detected in the gas phase at the outlet of the reactor or adsorbed in the materials, are reported in Table 3. With TiO_2-QZ, the compounds detected in the gas phase represent 72% relative to the amount of introduced DMS, with DMS as the main gaseous component, together with low amounts of dimethyldisulfide (DMDS) and only traces of dimethylsulfoxide (DMSO) and dimethylsulfone ($DMSO_2$). Carbon dioxide and water were only observed as sharp peaks at the very beginning of irradiation, and after 1 h for CO_2 and 5 h for H_2O, their concentration dropped and then stabilized at their initial value. Methanol and formaldehyde were also detected on the micro-TCD detectors. GC–MS analysis of the pre-concentrated gas flow on a Carboxen fiber additionally indicated the presence of trace amounts of formic acid, dimethyltrisulfide and methylmethanethiosulfonate (MMTS, $CH_3S(O)_2SCH_3$), together with an unidentified product (C_3H_8S).

In the case of ANT-SB, the amount of compounds detected in the gas phase is much lower (5%), with mainly DMS (3%), DMDS (1.4%), DMSO (0.6%) and traces of methanol. We also

Table 3
Organic products detected in the gas phase and by desorption of the irradiated materials in CH_2Cl_2 and acids detected by desorption in water in the case of DMS photocatalytic oxidation (bold characters: total yield relative to introduced DMS; italic characters: yield of specific compound relative to introduced DMS)

		TiO_2-QZ	ANT-SB	DCA-SG
Compounds detected in the gas phase under irradiation of DMS		**72 %** DMS (*67 %*) DMDS (*4 %*) DMSO (*1 %*) and traces of $DMSO_2$, CH_3OH, CH_2O, CO_2, H_2O, HCOOH, $CH_3S_3CH_3$, $CH_3S(O)_2SCH_3$, C_3H_8S	**5 %** DMS (*3 %*) DMDS (*1.4 %*) DMSO (*0.6 %*) and traces of CH_3OH and CO_2	**3 %** DMS (*2 %*) DMSO (*1 %*)
Compounds adsorbed in the material after irradiation of DMS	% products desorbed in CH_2Cl_2	**2 %** $DMSO_2$ (*0.5 %*) MMTS (*1.5 %*) traces of DMSO, DMDS, 2,3-dithiapentane	**20 %** $DMSO_2$ (*20 %*)	**29 %** DMSO (*17 %*) $DMSO_2$ (*11 %*) MMTS (*1 %*), Traces of DMDS
	% products desorbed in water	**3 %** Carboxylates (*1 %*) Sulfonates (*1 %*) Sulfates (*1 %*)	**3 %** Carboxylates (*0.1%*) Sulfonates (2.4 %) Sulfates (*0.5 %*)	**Traces** Sulfonates

observed a 2-fold increase of the CO_2 concentration as soon as the lamps were switched on.

With DCA-SG, only minor amounts of DMS and DMSO were found in the air flow all over the 120 h of irradiation (about 3% relative to introduced DMS). Neither carbon dioxide nor water was detected in this latter case.

It may be concluded that porous materials like DCA-SG and ANT-SB adsorb larger amounts of organic products and thus prevent their occurrence in the gas phase. In other words, with ANT-SB and DCA-SG, the air flow at the outlet of the reactor was almost totally decontaminated.

After irradiation, each material was desorbed in CH_2Cl_2 and then in water in order to analyze the adsorbed products. The results are also summarized in Table 3. For TiO_2-QZ, low amounts (2%) of $DMSO_2$ and MMTS, along with traces of DMDS, DMSO and 2,3-dithiapentane were detected in the organic extract. The products detected in the aqueous extract represented 3% of the initial starting amount, with formiate (1%), sulfonate (1%) and sulfate (1%) in similar proportion. High resolution XPS analysis of irradiated TiO_2-QZ confirmed the presence of a sulfate environment at the near surface [32]. With TiO_2-QZ, the overall material balance is 77%, not taking into account the amount of mineralized DMS.

On the contrary, with DCA-SG, organic products, mainly DMSO (17%), $DMSO_2$ (11%), and MMTS (1%) represented 29% of the introduced DMS and almost no acid (mainly sulfonates) desorbed from the silica monoliths in the aqueous extract. Highly polar DMSO and $DMSO_2$ interact strongly with silica sol–gel and hence accumulated on this material. These strongly absorbed products are probably not efficiently desorbed in CH_2Cl_2, which accounts for the poor material balance in this case (32%). Moreover, it may be noted that remaining physisorbed DMSO and $DMSO_2$ may be solubilized in water, but not quantified by ion chromatography. Another point of concern for this low material balance is the impossible DMS quantification in the organic extract due to overlapping with solvent chromatographic peak. It was however verified that only low DMS amounts were desorbed at 30 and at 100 °C from the irradiated material in a headspace thermodesorber coupled with a GC–MS. Hence, un-reacted DMS cannot account for the low material balance.

With ANT-SB, only $DMSO_2$ (20%) was recovered as organic product from silica beads. Several acids (3%), mainly sulfonate, were detected in the water extract. In this case too, the bad material balance probably arises from a poor desorption step in dichloromethane, and as previously, DMS cannot account for the missing products.

Another result worthy of note was the decrease of the intensity of the DRUV spectra of DCA-SG [32] and ANT-SB after irradiation (Fig. 3a and b, trace b). This intensity drop could be the consequence of either photosensitizer consumption under irradiation, or of the presence of adsorbed products which mask the photosensitizer spectra or the combination of both phenomena. It may first be noted that DCA, only included in the silica monolith DCA-SG, was totally recovered after desorption of the irradiated monoliths in CH_2Cl_2 as shown by the UV spectrum of the solution. This result implies that DCA

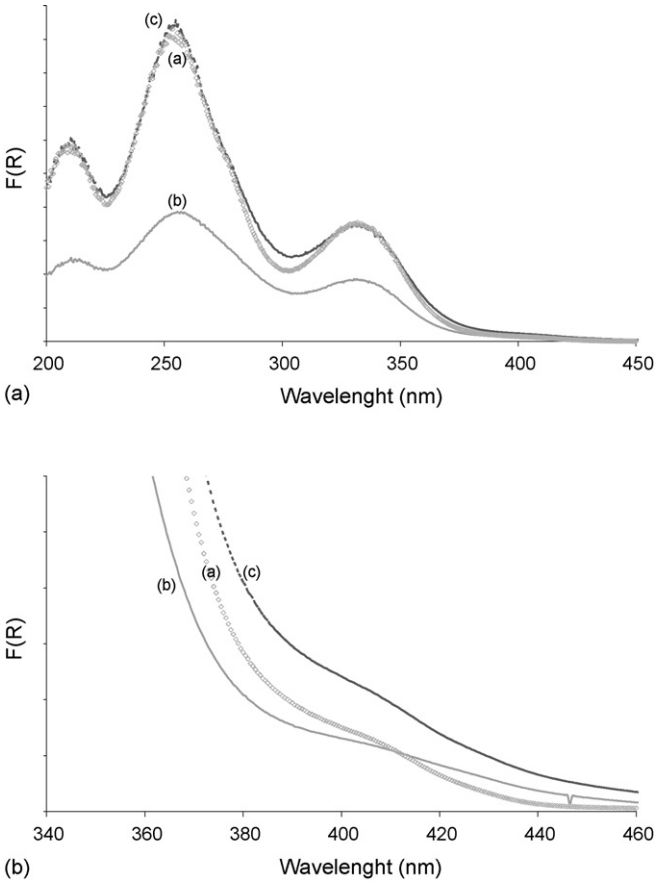

Fig. 3. (a) DRUV spectra (200–450 nm) of ANT-SB (a) before irradiation, (b) after irradiation under conditions of Entry 3 in Table 2 and (c) after regeneration by washing; (b) zoom (340–460 nm) of the same spectra.

was not consumed during oxidation process, but was easily desorbed by solvent washing of the material. Second, for ANT-SB, according to the UV analysis, no trace of anthraquinone was detected in the UV spectrum of the CH_2Cl_2 extract after irradiation, confirming the stability of the photosensitizer on the silica beads surface.

Many attempts were made in order to regenerate DCA-SG, but none of them was successful (in the better case, the photoactivity was divided by 2) [32]. To solve the problem of the regeneration, the grafting of the photosensitizer (PS) was developed and led to the elaboration of ANT-SB. Contrary to DCA-SG, the photosensitizer was chemically bound to the silica support and thus the material could be washed without loss of the PS as seen above.

The regeneration of ANT-SG was followed and evaluated by DRUV spectroscopy (Fig. 3a and b). The photocatalyst was washed, after the photooxidation experiment of Entry 3 (Table 2), first in CH_2Cl_2 and second in H_2O. Then, it was dried under primary vacuum at 100 °C for 2 h. This regenerated material could be re-used for DMS photoxidation in the same process conditions than Entry 3 of Table 2, without any efficiency drop, as deduced from DMS removal (98% DMS abatement with either original ANT-SB or regenerated ANT-SB). This result was further confirmed by DRUV analysis. After regeneration, the DRUV spectra of the original and regenerated

Table 4
Efficiency for DMDS removal of each photocatalyst under various conditions

Entry	Photocatalyst used	Irradiation wavelength (nm)	Flow rate (ml min^{-1})	Gas hourly space velocity (GHSV) (h^{-1})	DMDS concentration (ppmv)	% DMDS abatement
5	DCA-SG, 0.67 g	420	67	2250	100	15
6	ANT-SB, 1 g	420	20	336	50	45
7	TiO_2-QZ, 1 g	350	20	269	50	18

ANT-SB were identical with a recovered intensity of the band between 400 and 440 nm (Fig. 3a and b, traces a and c). We can thus conclude that the presence of oxidation products in the material was responsible for the intensity drop of the DRUV spectra after irradiation and that no PS consumption occurred during irradiation. Other photooxidation experiments were performed with ANT-SB by successive cycles irradiation–washing–drying and revealed a long lifetime for this material.

5.2.2. DMDS

The results concerning the efficiency of each material for DMDS removal are summarized in Table 4. With DCA-SG, under the conditions previously used for DMS (Entry 1, Table 2), with the highest GHSV (2250 h^{-1}), only poor DMDS abatement was achieved (15%, Entry 5) instead of 90% for DMS (Table 2, Entry 1). This result implies that DMDS removal rate was slower than DMS removal rate, using DCA-SG as photocatalyst. Accordingly in the following, reaction conditions were changed in order to optimize DMDS photodegradation. The flow rate was decreased from 67 to 20 ml min^{-1} and the inlet DMDS concentration divided by 2 while the photocatalyst weight was increased from 0.67 to 1 g (Table 4).

Under these conditions, with a lower GHSV (from 2250 to 336 and 269 h^{-1}), ANT-SB showed a better photocatalytic activity on DMDS abatement (45% DMDS removal; Entry 6) than TiO_2-QZ (18% DMDS removal; Entry 7). The oxidation products arising from DMDS are presented in Table 5.

With DCA-SG, under un-optimized conditions, 78% of the introduced DMDS was recovered in the air flow at the outlet of the reactor: mainly DMDS (77%) and only low amounts of methyl methanethiosulfonate (MMTS) and dimethyltrisulfide (DMS_3) were observed. With TiO_2-QZ, even with a lower GHSV, the same compounds were detected in the air flow in a higher extent (81% of the total amount): un-reacted DMDS (70%) and DMS_3 (11%). With ANT-SB, these products were detected in lower amounts (50% of introduced DMDS) with still DMDS as the main product. In the three cases, no significant increase of CO_2 and H_2O concentrations was observed.

Desorption was then carried out for the three materials with CH_2Cl_2 and with H_2O. The obtained results are also presented in Table 5.

First of all, for the three materials, un-reacted DMDS was recovered in low amounts from desorption in CH_2Cl_2. For the three materials, MMTS appears to be the main adsorbed compound, with highest yield on DCA-SG, together with traces of trisulfide DMS_3 and $C_3H_8S_3$ (methyl(methylthio)methyldisulfide ($CH_3SCH_2SSCH_3$)). It may be pointed out that MMTS formation increased in the order TiO_2-QZ (5%), ANT-SB (15%), and DCA-SG (20%).

In the aqueous extracts, sulfonates were always the main desorbed acids, with highest yield from ANT-SB and lowest yield from DCA-SG as seen previously with DMS. Sulfates are also detected as noticeable by-products (5%) starting from TiO_2-QZ.

ANT-SB thus displays the highest efficiency for DMDS oxidation relative to TiO_2-QZ and DCA-SG (with DCA-SG, operating conditions such as GHSV and inlet concentration, were much less favourable), with main formation of sulfonate (27%) and MMTS (15%). Selective formation of MMTS thus occurred with DCA-SG while acids and especially sulfates were preferably obtained with TiO_2-QZ. In this latter case, the ratio of DMS_3 and $C_3H_8S_3$ in the organic products is the highest. As for DMS, ANT-SB displayed an intermediate reactivity, between TiO_2-QZ and DCA-SG.

With the three materials, the overall material balance is much better for DMDS than for DMS. This probably results from the lower affinity of the oxidation products (MMTS, DMS_3) with the silica matrix. Moreover, in this case un-reacted DMDS is easily quantified by chromatography.

6. Discussion

From the results described above, the efficiency of immobilized sensitizers to oxidize both dimethylsulfide (DMS) and dimethyldisulfide (DMDS) at the gas–solid interface is demonstrated.

For DMS removal, the cleanest air flow is obtained by irradiation of DCA-SG at 420 nm: with this material, almost no oxidation product, except traces of DMSO, is detected in the effluent for more that 120 h. Two explanations may be put forward to account for the high efficiency of DCA-SG. First, the major oxidation product is a highly polar, partially oxidized compound, dimethylsulfoxide, arising from the fast addition of singlet oxygen on dimethylsulfide [32].

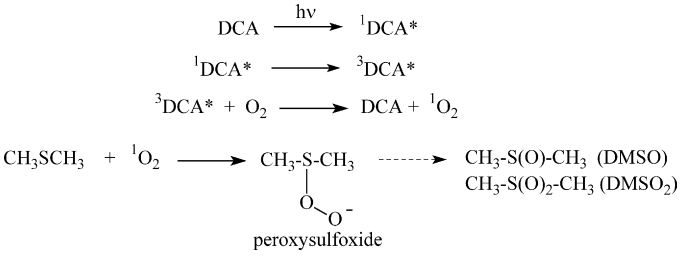

Second, due to their high specific surface area, the sol–gels are the most adsorbing materials. Accordingly, almost all the dimethylsulfoxide remains adsorbed on the catalyst.

On the contrary, for DMS removal with TiO_2-QZ, in the absence of water, large amounts of starting sulfide and of

Table 5
Organic products detected in the gas phase and by desorption of the irradiated materials in CH_2Cl_2 and acids detected by desorption in water in the case of DMDS photocatalytic oxidation (bold characters: total yield relative to introduced DMS; italic characters: yield of specific compound relative to introduced DMS). DMS_3: CH_3SSSCH_3; $C_3H_8S_3$: methyl(methylthio)methyldisulfide ($CH_3SCH_2SSCH_3$)

		TiO_2-QZ	ANT-SB	DCA-SG
Compounds detected in the gas phase under irradiation of DMDS		**81 %** DMDS (*70 %*) DMS_3 (*11 %*) MMTS (*traces*)	**50 %** DMDS (*47 %*) DMS_3 (*3 %*) MMTS (*traces*)	**78 %** DMDS (*77 %*) DMS_3 (*1%*) MMTS (*traces*)
Compounds adsorbed in the material after irradiation of DMDS	% products desorbed in CH_2Cl_2	**8 %** DMDS (*2 %*) DMS_3 (*1%*) MMTS (*5 %*) $C_3H_8S_3$ (*traces*)	**19 %** DMDS (*3 %*) DMS_3 (*1 %*) MMTS (*15 %*) $C_3H_8S_3$ (*traces*)	**20 %** MMTS (*20 %*) DMDS, DMS_3, $C_3H_8S_3$ (*traces*)
	% products desorbed in water	**11 %** Carboxylates (*1 %*) Sulfonates (*5 %*) Sulfates (*5 %*)	**31 %** Carboxylates (*2 %*) Sulfonates (*27 %*) Sulfates (*2 %*)	**2 %** Carboxylates (*traces*) Sulfonates (*2 %*) Sulfates (*traces*)

disulfide are detected at the outlet of the reactor, even if mineralization is shown to partially occur from the detection of acids, carbon dioxide and water. These results are consistent with the literature data, where disulfide was observed in large amount in dry air [16]. In the absence of water, and hence of hydroxyl radicals, the formation of products arising from the cleavage of the C–S bond (such as disulfide, DMDS) can only be accounted for by radical pathways, well known for sulfur radical cation [45]. On the other hand, addition of superoxide anion on radical–cation actually may account for the formation of DMSO and $DMSO_2$, only detected in minor amounts in this case.

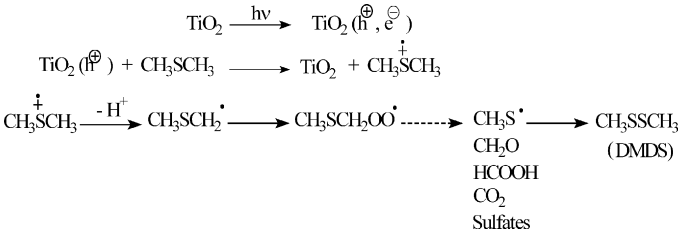

With ANT-SB, the effluent is as decontaminated as with DCA-SG and DMDS is detected as the main by-product in the gas phase, already observed in the case of TiO_2-QZ. The only adsorbed organic product detected in this case is $DMSO_2$. This result can tentatively be assigned to competitive pathways, with both singlet oxygen formation and addition towards dimethylsulfone on one hand, and radical mechanism through electron transfer reaction and carbon sulfur bond cleavage on the other hand.

For DMDS removal, the overall efficiency of the three materials is lower than for DMS, despite the adsorption capacity in the same range for the three materials for both pollutants. Under the same operating conditions (air flow, inlet concentration, GHSV), with DCA-SG, while DMS abatement is 90%, it decreases to 15% for DMDS. With ANT-SB and TiO_2-QZ, DMDS abatement reaches only 45 and 18%, respectively, while DMS abatement is 98 and 30% with higher GHSV and higher inlet concentrations, i.e. less favourable reaction conditions. This result proves that at the gas–solid interface, the kinetic of the DMDS photooxidation reaction is slower than that of DMS. The same conclusion was also drawn from previous studies in solution [45] and from the results of Nishikawa and Takahara [13]. This weaker reactivity of DMDS appears surprising, when taking into account the redox potentials: 1.79 V for DMS and 1.15 V for DMDS versus SCE in CH_3CN, from which it follows that oxidation of DMDS through electron transfer should be thermodynamically favoured relative to that of DMS [43]. On the other hand, in solution, singlet oxygen addition on disulfides leading to thiosulfonates occurs much less readily than its addition on sulfides [43,50], as observed here at the gas–solid interface. Further kinetic studies aimed at a better understanding of this observation are currently in progress.

Another point of concern is the detection of previously undetected intermediates arising from DMDS oxidation with TiO_2-based materials. According to Canela et al., with a relative RH 23% [12], and Nishikawa and Takahara [13], only carbon dioxide, sulfur dioxide, adsorbed sulfate, formic and acetic acid were obtained under their conditions. Under our conditions (high GHSV, low catalyst loading, absence of water), we demonstrate the presence of dimethyltrisulfide, methyl(-methylthio)methyldisulfide ($CH_3SCH_2SSCH_3$) and methyl methane thiosulfonate (MMTS). The two former products may only be accounted for by C–S, S–S and C–H bond cleavage, i.e. radical mechanism without any possible formation of hydroxyl radical, while thiosulfonate may arise from singlet oxygen addition as already demonstrated in solution [50].

Both mechanisms (electron transfer and singlet oxygen addition) are probably involved with ANT-SB, as deduced from the distribution of reaction products from DMDS as from DMS.

Grafting of the photosensitizer molecule on the silica network greatly improves its stability and allows several cycles irradiation–washing–drying, without oxidation or leak of the photosensitizer molecule, as demonstrated by the DRUV spectra of the material and steady oxidation efficiency. These results at the gas–solid interface nicely confirm the already described solution reactivity of anthraquinone [45].

Despite the very low amount of photosentizing molecules for both materials (2.1×10^{-7} mol g^{-1} for DCA-SG and 2.8×10^{-4} mol g^{-1} for ANT-SB), they are at least as efficient as TiO_2, under low RH conditions.

7. Conclusion

Photosensitizer-based materials have proven their efficiency for DMS and DMDS oxidation at the gas–solid interface and present several advantages relative to TiO_2-based materials: they are activated by visible light, transparent, highly porous and easily handled in a gas phase reactor. A thorough identification of the obtained products and their tentative quantification was carried out for two different materials, by comparison with a TiO_2-based material. From product distribution, the involved mechanisms appear to be different from those generally described for TiO_2 photocatalysis: mineralization is not possible but rather partial oxidation through singlet oxygen addition to intermediate oxygenated products, strongly retained on silica. On the other hand, under the conditions used in this study (low catalyst loading, high GHSV, absence of water), with the TiO_2-based material, incomplete mineralization of DMS and no mineralization of DMDS is observed, whereas a number of by-products are identified especially in the DMDS case. These products are indicative of electron transfer from DMS or DMDS to the photogenerated hole, followed by radical mechanisms.

For the PS-based materials, if the photosensitizer is grafted on the silica support, they can be easily regenerated by desorption of polar oxidation products in suitable solvents, and be re-used without loss of efficiency. Such photosensitizing materials, leading to partial oxidation, may be used for decontamination purpose, in complement to conventional TiO_2-based photocatalysis. Further work aimed at the elaboration of stable material where different photosensitizing molecules are grafted is currently under progress in order to widen the possible range of applications. Photocatalytic studies under different conditions (GHSV, RH, temperature, ...) are also being undertaken.

Acknowledgements

The authors acknowledge A. Koukh (University of Pau) for recording NMR spectra. The authors also gratefully acknowledge the financial support of Agence De l'Environnement et de la Maîtrise de l'Energie (ADEME) for this study and the Centre Technique du Papier for technical collaboration.

References

[1] S. Sivela, in: L. Simons (Ed.), Commentationes Physico-Mathematicae, Dissert. No. 1, Societas Scientarium Fennica, Helsinki, 1980, p. 1.
[2] M. Lewandoski, D.F. Olis, Mol. Supramol. Photochem. 10 (2003) 249 (semiconductor photochemistry and photophysics).
[3] J. Peral, X. Domenech, D.F. Ollis, J. Chem. Technol. Biotecnol. 70 (1997) 117.
[4] D.M. Blake, NREL/TP-510-31319 (2001). Available electronically at http://www.osti.gov/bridge.
[5] J. Peral, D.F. Ollis, J. Mol. Catal. A 115 (1997) 347.
[6] N. Gonzalez-Garcia, J. Ayllon, X. Domenech, J. Peral, Appl. Catal. B 52 (2004) 69.
[7] A.V. Vorontsov, A.E.N. Savinov, L. Davydov, P.G. Smirniotis, Appl. Catal. B 32 (2001) 11.
[8] A.V. Vorontsov, A.A. Panchenko, E.N. Savinov, C. Lion, P.G. Smirniotis, Environ. Sci. Technol. 36 (2002) 5621.
[9] A.V. Vorontsov, C. Lion, E.N. Savinov, G. Smirniotis, J. Catal. 220 (2003) 414.
[10] I.N. Martyanov, K.J. Klabunde, Environ. Sci. Technol. 37 (2003) 3448.
[11] D.A. Panayotov, D.K. Paul, J.T. Yates, J. Phys. Chem. 107 (2003) 10571.
[12] M.C. Canela, R.M. Alberici, R.C. Sofia, W.F. Jardim, Environ. Sci. Technol. 33 (1999) 2788.
[13] H. Nishikawa, Y. Takahara, J. Mol. Catal. A 172 (2001) 247.
[14] A.V. Vorontsov, A.E.N. Savinov, C. Lion, P.G. Smirniotis, Appl. Catal. B 44 (2003) 25.
[15] D.V. Kozlov, A.V. Vorontsov, P.G. Smirniotis, E.N. Savinov, Appl. Catal. B 42 (2003) 77.
[16] K. Demeestere, J. Dewulf, B. De Witte, H. Van Langenhove, Appl. Catal. B: Environ. 60 (2005) 93.
[17] K. Demeestere, J. Dewulf, T. Ohno, P.H. Salgado, H. Van Langenhove, Appl. Catal. B: Environ. 61 (2005) 140.
[18] R. Asahi, T. Morikawa, T. Ohwaki, K. Aoki, Y. Taga, Science 293 (2001) 269.
[19] T. Morikawa, R. Asahi, T. Ohwaki, K. Aoki, Y. Taga, Jpn. J. Appl. Phys. 40 (2001) L561.
[20] T. Ihara, M. Miyoshi, Y. Iriyama, O. Matsumoto, S. Sugihara, Appl. Catal. B: Environ. 42 (2003) 403.
[21] S. Yin, Q. Zhang, F. Saito, T. Sato, Chem. Lett. 32 (2003) 358.
[22] T. Lindgren, J.M. Mwabora, E. Avendano, J. Jonsson, A. Hoel, C.-G. Granqvist, S.-E. Lindquist, J. Phys. Chem. B 107 (2003) 5709.
[23] S. Sakthivel, H. Kisch, Chem. Phys. Chem. 4 (2003) 487.
[24] H. Irie, S. Washizuka, N. Yoshino, K. Hashimoto, Chem. Commun. (2003) 1298.
[25] K. Kobayakawa, Y. Murakami, Y. Sato, J. Photochem. Photobiol. A: Chem. 170 (2005) 177.
[26] C. Lettmann, K. Hildenbrand, H. Kisch, W. Macyk, W.F. Maier, Appl. Catal. B: Environ. 32 (2001) 215.
[27] S. Sakthivel, H. Kisch, Angew. Chem. Int. Ed. 42 (2003) 4908.
[28] T. Ohno, T. Tsubota, K. Nishijima, Z. Miyamoto, Chem. Lett. 33 (2004) 750.
[29] T. Umebayashi, T. Yamaki, S. Yamamoto, A. Miyashita, S. Tanaka, T. Sumita, K. Asai, J. Appl. Phys. 93 (2003) 5156.
[30] T. Umebayashi, T. Yamaki, S. Tanaka, K. Asai, Chem. Lett. 32 (2003) 330.
[31] T. Ohno, M. Akiyoshi, T. Umebayashi, K. Asai, T. Mitsui, M. Matsumura, Appl. Catal. A: Gen. 265 (2004) 115.
[32] C. Cantau, T. Pigot, R. Brown, P. Mocho, M.T. Maurette, F. Benoit-Marquié, S. Lacombe, Appl. Catal. B: Environ. 65 (2006) 77.
[33] X.Z. Li, M.F. Hou, F.B. Li, H. Chua, Ind. Eng. Chem. Res. 45 (2006) 487.
[34] S. Kato, Y. Hirano, M. Iwata, T. Sano, K. Takeuchi, S. Matsuzawa, Appl. Catal. B: Environ. 57 (2005) 109.
[35] M. Cohen-Atiya, D. Mandler, J. Electroanal. Chem. 550 (2003) 267.
[36] P.E. Laibinis, G.M. Whitesides, D.L. Allara, Y. Tao, A.N. Parikh, R.G. Nuzzo, J. Am. Chem. Soc. 113 (1991) 7152.
[37] C.H. Liu, L. Zhang, Y. He, Thin Solid Films 304 (1997) 13.
[38] M.C. Canela, R.M. Alberici, W.F. Jardim, J. Photochem. Photobiol. A 112 (1998) 73.
[39] S. Kataoka, E. Lee, M.I. Tejedor-Tejedor, M.A. Anderson, Appl. Catal. B: Environ. 61 (2005) 159.
[40] D. Wöhrle, O. Suvorova, R. Gerdes, O. Bartels, L. Lapok, N. Baziakina, S. Makarov, A. Slodek, J. Porphyrins Phthalocyanines 8 (2004) 1020.
[41] D. Wöhrle, N. Baziakina, O. Suvorova, S. Makarov, V. Kutureva, E. Schupak, G. Schnurpfeil, J. Porphyrins Phthalocyanines 8 (2004) 1390.
[42] N. Soggiu, H. Cardy, J.L. Habib-Jiwan, I. Leray, J.Ph. Soumillion, S. Lacombe, J. Photochem. Photobiol. A: Chem. 124 (1999) 1.
[43] S. Lacombe, H. Cardy, M. Simon, A. Khoukh, J.Ph. Soumilllion, M. Ayadim, Photochem. Photobiol. Sci. 1 (2002) 347.
[44] V. Latour, T. Pigot, P. Mocho, S. Blanc, S. Lacombe, Catal. Today 101 (2005) 359.

[45] V. Latour, T. Pigot, H. Cardy, M. Simon, S. Lacombe, Photochem. Photobiol. Sci. 4 (2005) 221.
[46] F. Benoit-Marquié, M.T. Boisdon, A.M. Braun, E. Oliveros, M.T. Maurette, Entropie 228 (2000) 36.
[47] F. Benoit-Marquié, U. Wilkenhöner, V. Simon, A.M. Braun, E. Oliveros, M.T. Maurette, J. Photochem. Photobiol. A 132 (2000) 225.
[48] S. Lacombe, H. Cardy, N. Soggiu, S. Blanc, J.L. Habib-Jiwan, J.Ph. Soumillion, Micropor. Mesopor. Mater. 46 (2001) 311.
[49] Gas hourly space velocity (GHSV, h^{-1}) is defined as the ratio of the flow rate ($m^3\ h^{-1}$) on the catalyst volume (m^3). This parameter is more relevant in the case of granular material as suggested in *Manual on Catalyst Characterization* (J. Haber, Pure Appl. Chem., vol. 63 (9) (1991) 1227–1249). Most often, in the literature described in the review section, residence time (s) is defined as the reciprocal of GHSV.
[50] E.L. Clennan, D. Wang, H. Zhang, C.H. Clifton, Tetrahedron Lett. 40 (1994) 4723.